

# Enhancement of the compressive strength of highly porous $\text{Al}_2\text{O}_3$ foam through crack healing and improvement of the surface condition by dip-coating

Rizwan Ahmad<sup>a,b</sup>, Jang-Hoon Ha<sup>a</sup>, In-Hyuck Song<sup>a,b,\*</sup>

<sup>a</sup>Engineering Ceramic Department, Korea Institute of Materials Science, 797 Changwondaero, Seongsan-gu, Changwon, Gyeongnam 642-831, Republic of Korea

<sup>b</sup>University of Science and Technology (UST), 217, Gajeong-ro, Yuseong-gu, Daejeon 305-350, Republic of Korea

Received 26 August 2013; received in revised form 13 September 2013; accepted 13 September 2013

Available online 20 September 2013

## Abstract

Highly porous ceramic foams with open or closed cells have a wide variety of industrial applications, such as high-temperature filtration, absorption, catalyst support, lightweight materials, and high-temperature structural components. The mechanical strength of these highly porous ceramics decreases when the porosity in the foam reaches 90%. This work investigated the preparation of a highly porous  $\text{Al}_2\text{O}_3$  substrate with a porosity of approximately 90% using a direct foaming technique, and coatings were deposited onto the substrate using  $\text{Al}_2\text{O}_3$  slips prepared with powders of different particle sizes via a dip-coating process. Upon coating the surfaces of the foam, the surface condition was improved, and cracks were healed, producing a versatile material with good compressive strength. The interface between the  $\text{Al}_2\text{O}_3$  coatings with different particle sizes and the substrate was analysed by observing the microstructure of the specimens, and their compressive strengths were compared with the compressive strength of an uncoated specimen after sintering at 1600 °C and 1700 °C for 1 h.

© 2013 Elsevier Ltd and Techna Group S.r.l. All rights reserved.

**Keywords:** Porous ceramics; Dip-coating; Alumina; Compressive strength

## 1. Introduction

The performance of engineered porous ceramic materials is gauged by their high-temperature stability, low weight, high porosity, low thermal conductivity, and good mechanical strength. These properties have led to a diverse range of applications, including solid oxide fuel cell insulators [1], metal melt filtration, ion-exchange filtration, heat exchangers, refractory linings, and catalyst supports [2]. Highly porous ceramic foams with open or closed cells are good candidates to be heat-shielding materials but exhibit poor mechanical strength when the porosity in the foams reaches 90%. Mostly porous materials are prone to debris problems, and certain applications require an insulation material without debris to ensure a clean environment.

The mechanical strength of highly porous materials can be enhanced by coating their surfaces. Son et al. [3] investigated a vacuum slurry coating technique during the fabrication of a dense and thin electrolyte coating on the surface of a porous anode for SOFC applications, whereas Lan et al. [4] studied the fabrication of thick yttria-stabilised-zirconia coatings with thicknesses up to 420  $\mu\text{m}$  via the pressure infiltration of slurry for use as a thermal barrier coating for high-temperature applications. Coatings have been used to protect manufactured components from thermal or corrosive degradation and to impart good wear resistance and hardness to surfaces. There are several coating techniques that are currently employed, among which dip-coating is a simple and cost-effective method that has been optimised by many researchers [5–8] to fabricate both porous and dense ceramic coatings. This method offers good flexibility when used to coat components with complex geometries, and the uniform coating of large areas as well as controllable film thicknesses can be ensured by dip-coating. Gu et al. [9] presented a model of the fabrication of a uniform ceramic membrane by a dip-coating technique. In the

\*Corresponding author at: Engineering Ceramic Department, Korea Institute of Materials Science, 797 Changwondaero, Seongsan-gu, Changwon, Gyeongnam 642-831, Republic of Korea. Tel.: +82 55 280 3534; mobile: +82 10 5584 4843.

E-mail address: [sih1654@kims.re.kr](mailto:sih1654@kims.re.kr) (I.-H. Song).



dip-coating process, the driving force for film formation is the capillary force of the porous substrate. The capillary force generated by touching the substrate to the meniscus of the slip yields a uniform coating thickness over a porous substrate. As the capillary force increases, the porous surface is effectively coated, thus reducing the effect of surface defects of the substrate on the coating properties [9]. In the dip-coating process, a substrate is immersed in a suspension with an appropriate rheology and is then withdrawn at a constant rate. The deposited wet film, upon drying and sintering, transforms into a solid film that adheres to the substrate.

A particle-stabilised direct foaming technique developed by Gonzenbach et al. [10–12] based on in situ hydrophobisation of colloidal particles was used to prepare a highly porous  $\text{Al}_2\text{O}_3$  substrate. In this technique, bubbles are incorporated into a suspension containing surfactant-modified, partially hydrophobic particles that attach themselves to the air/water interface and create a protective shield around the bubbles. The high stability of particle-stabilised foams is attributed to the irreversible adsorption of partially hydrophobic particles at the air/water interface, which impedes destabilisation mechanisms such as coalescence, drainage, and Ostwald ripening [13–15].

Lange et al. [16] healed surface cracks in polycrystalline alumina by heating specimens to a high temperature for a short period; however, the crack-healing behaviour of highly porous  $\text{Al}_2\text{O}_3$  prepared through a particle-stabilised direct foaming technique has not been studied. In the present study, we elucidated the effect of coating on the microstructure and compressive strength of a highly porous  $\text{Al}_2\text{O}_3$  foam manufactured by the particle-stabilised direct foaming technique. The particle-stabilised  $\text{Al}_2\text{O}_3$  foam was dip-coated with aqueous slips prepared with  $\text{Al}_2\text{O}_3$  powders of different particle sizes to produce a material with a macroporous substrate and a microporous coating. The inhomogeneities on the surface and cracks were healed by the dip-coating process to improve the compressive strength and enhance the debris resistance of the highly porous foam, which can be efficiently used as a heat-shielding material in applications that require an environment free of contamination.

## 2. Experimental procedures

Commercially available  $\alpha\text{-Al}_2\text{O}_3$  (AKP-30, Sumitomo Chemicals Co. Ltd., Japan) with a particle size of 0.3–0.5  $\mu\text{m}$  and a BET surface area of 5–10  $\text{m}^2/\text{g}$  was used for the preparation of the substrate. Aqueous colloidal suspensions were initially prepared with 50 vol% solid loading, and 2 N HCl was used for the electrostatic dispersion of the particles, followed by ball milling for 24 h with a ball-to-powder volume ratio of 2:1. Valeric acid (99% pure, Sigma-Aldrich) was diluted in water to obtain a final solid loading of 35 vol%; the solution was added dropwise immediately after ball milling for the in situ hydrophobisation of the  $\text{Al}_2\text{O}_3$  particles. The final pH of the slurry was adjusted to 4.7 using a 1 N NaOH solution, and foaming was carried out using a direct drive motor at a rotational speed of 1000 rpm. The specimens were prepared by using Perspex moulds, followed by drying for 24 h in a

humidity- and temperature-controlled chamber at 20 °C with a humidity level of 90%. After 24 h, the temperature was increased to 30 °C while the humidity remained at 90%. Sintering of the specimens was carried out at 1600 °C at a heating rate of 1 °C/min and a dwell time of 2 h. After sintering, the specimens were cut and used as substrates to be coated with different particle sizes  $\text{Al}_2\text{O}_3$ .

Aqueous  $\text{Al}_2\text{O}_3$  slips were prepared with AKP-30 and ALM-44 (Sumitomo Chemicals Co. Ltd., Japan) with a solid loading of 50 wt%. HS dispersant 5802 (SAN NOPCO KOREA LTD.) was added to 2 wt% water to disperse the  $\text{Al}_2\text{O}_3$  particles. HS-BD 25 (SAN NOPCO KOREA LTD.) was added to 10 wt% of water to form a binder. The slips were ultrasonicated for 1 h to ensure dispersion of the particles in water. Prior to the coating process, the substrate surfaces were smoothed by carefully rubbing on a fine silicon carbide abrasive paper. The substrates were coated with AKP-30 and ALM-44 by dipping them into the slips for 5 s and withdrawing at a speed of 4 mm/s. Additional coatings were applied by re-dipping the previously dip-coated and dried specimens at 30 °C. The resulting specimens were finally dried at 30 °C for 24 h and sintered at 1600 °C and 1700 °C at a heating rate of 3 °C/min and a dwell time of 1 h.

The particle size distribution of the initial powders was determined using a particle size analyser (Beckman Coulter LST<sup>TM</sup> 13 320 Laser diffraction particle size analyser, USA). Microstructural analysis of the final specimens was performed using SEM (JSM-5800, JEOL, Tokyo, Japan). The compressive strength of the specimens coated on all sides (10 mm  $\times$  10 mm  $\times$  10 mm in size) was measured using a uni-axial mechanical tester (Instron Corporation) connected to a software “Series IX Automated Materials Testing System”. A load cell of 500 kg<sub>f</sub> was used and crosshead speed was 0.5 mm/s. Five specimens under each condition of coating were tested to obtain the mean and standard deviation.

## 3. Results and discussion

The results of the particle size analysis of the  $\text{Al}_2\text{O}_3$  powders are shown in Fig. 1. AKP-30 showed a small particle size  $D_{50}$  of 0.3  $\mu\text{m}$  with a narrow distribution, whereas ALM-

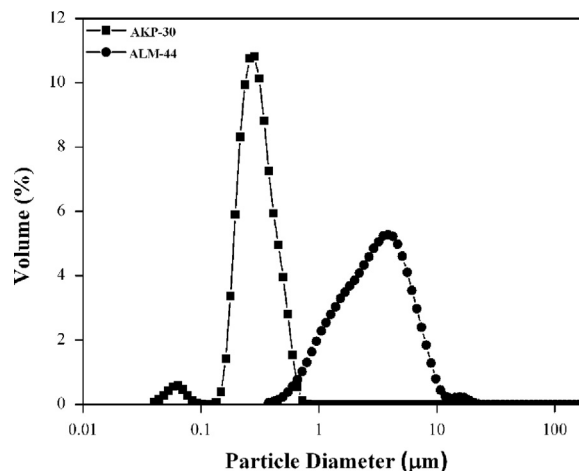


Fig. 1. Particle size analysis of the starting  $\text{Al}_2\text{O}_3$  powders.



44 showed a large particle size  $D_{50}$  of 3.148  $\mu\text{m}$  with a wide distribution. AKP-30 was used for the preparation of the substrate because a submicron particle size is more suitable for particle-stabilised direct foaming. The fractured surface of the  $\text{Al}_2\text{O}_3$  substrate sintered at 1600  $^\circ\text{C}$  for 2 h, demonstrating the

cell morphology and porosity, is shown in Fig. 2(a). The cell size of the substrate ranged from 70 to 200  $\mu\text{m}$  with a porosity of approximately 90%. This porosity of the  $\text{Al}_2\text{O}_3$  foam substrate was determined from the ratio of the bulk density to the theoretical density, and the bulk density of the substrate

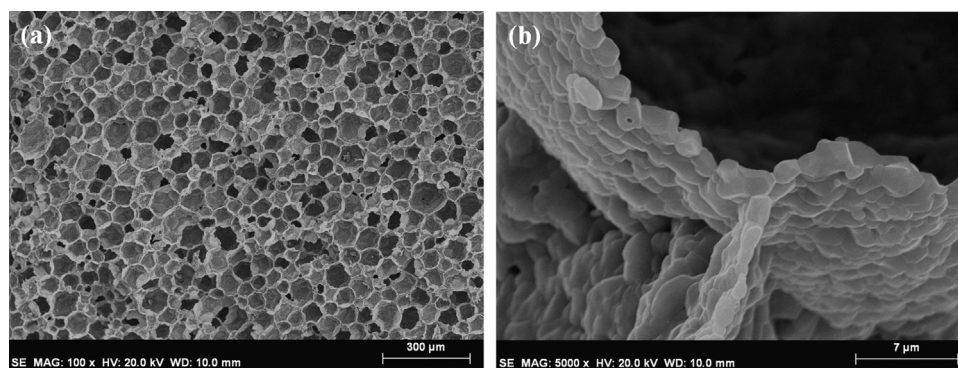


Fig. 2. SEM images of the  $\text{Al}_2\text{O}_3$  foam substrate sintered at 1600  $^\circ\text{C}$  for 2 h (a) showing uniform cell size and cell morphology and (b) a single strut wall.

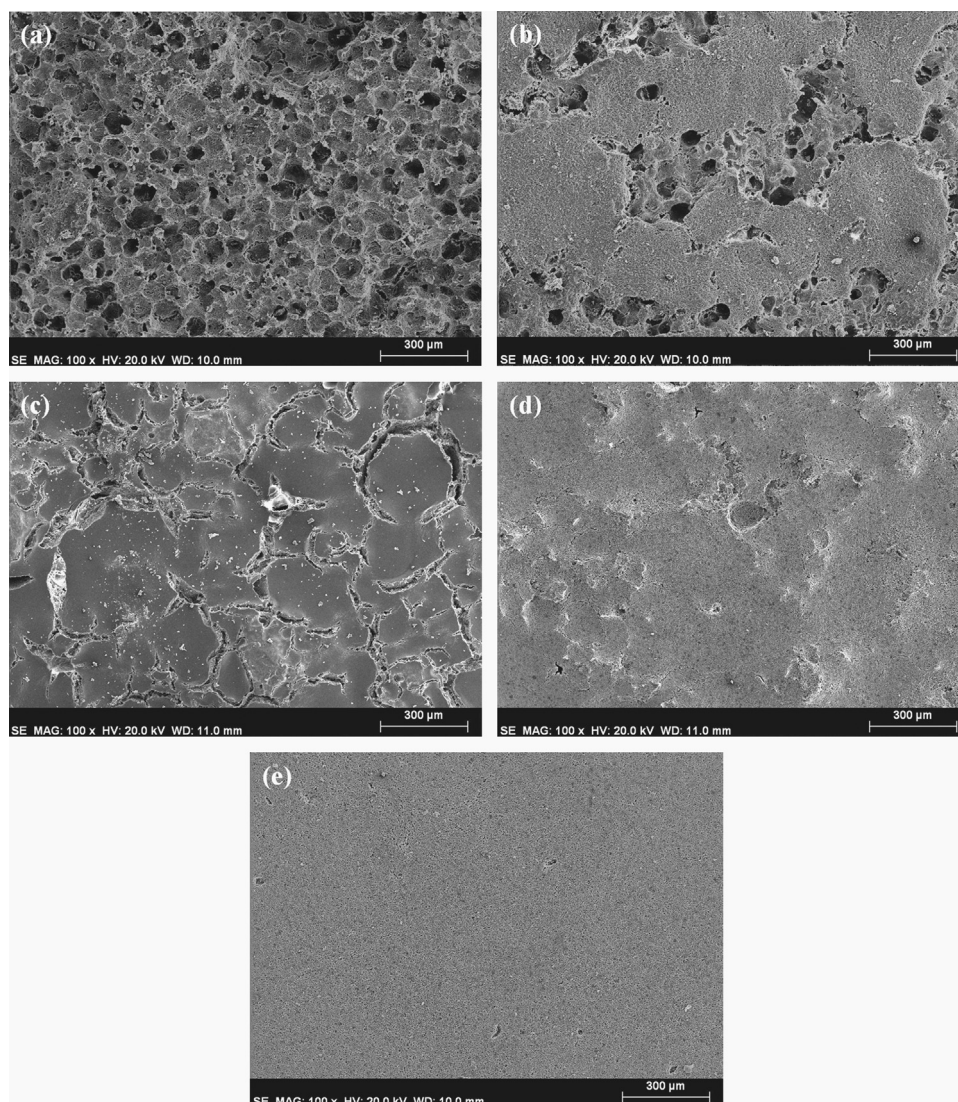


Fig. 3. SEM images of the AKP-30 coating surface sintered at 1600  $^\circ\text{C}$  for 1 h: (a) coated twice, (b) coated three times, (c) coated four times, (d) coated five times, and (e) coated five times with the ALM-44 sintered at 1600  $^\circ\text{C}$  for 1 h.



was calculated from the mass-to-volume ratio. The substrate manufactured by the particle-stabilised direct foaming method exhibited a unique single strut wall, as shown in Fig. 2(b). Through this method, the surface of the  $\text{Al}_2\text{O}_3$  particles was altered to become partially hydrophobic by adsorbing valeric acid on the surface of the particles. The pH of the  $\text{Al}_2\text{O}_3$  colloidal system was maintained at 4.7 to obtain a higher zeta potential because the IEP value of  $\text{Al}_2\text{O}_3$  is approximately 9. At pH 4.7,  $\text{Al}_2\text{O}_3$  exhibited the positive surface ion  $\text{AlOH}_2^+$ , and valeric acid deprotonated into  $\text{CH}_3\text{--CH}_2\text{--CH}_2\text{--CH}_2\text{--COO}^-$  and  $\text{H}^+$  ions. The anion ( $\text{CH}_3\text{--CH}_2\text{--CH}_2\text{--CH}_2\text{--COO}^-$ ) of valeric acid is capable of getting adsorbed electrostatically onto the cationic surface of  $\text{Al}_2\text{O}_3$  particles to render them partially hydrophobic by leaving their tails in the aqueous solution. These surface-modified, partially hydrophobic  $\text{Al}_2\text{O}_3$  particles are adsorbed irreversibly on the air/water interface to stabilise the foam.

Aqueous slips were prepared with AKP-30 and ALM-44 powders and used to coat the substrates. An  $\text{Al}_2\text{O}_3$  foam substrate shows good wettability toward an aqueous slip, thus producing a uniform coating.  $\text{Al}_2\text{O}_3$  foam prepared utilizing the particle-stabilised direct foaming technique has inherently closed cells but the cell openings are most likely formed by local differential shrinkage of the particle layer around bubbles during drying. This shrinkage favored rupture of the particle coating around the bubbles, leading to interconnectivity of cells after drying and sintering. Therefore, our foam specimens have both open and closed cells. In the dip-coating process, a substrate is immersed in a ceramic slip, which contains a dispersant and a binder and is then withdrawn at a constant rate. When the specimens were dipped into the suspensions, the ceramic particles in the suspension were deposited on the surface of the specimens due to capillary force which acts as a driving force for coating and also penetrated into the cracks to heal them. Therefore, the effect of particle size was studied on the healing of cracks and improvement in the compressive strength. For a microporous substrate, the capillary force is high and the porous surface will be coated effectively. However, in this study, a macroporous substrate was used, which induces a lower capillary force relative to that induced by a microporous substrate, thus creating a lower driving force for coating. If the capillary force is not sufficient, the coating

layer will have several defects, such as uncoated areas, pores, cracks, and pinholes, as shown in Fig. 3. For AKP-30 and ALM-44, five coatings were required to obtain a uniform coating on the substrates, whereas cracks and non-uniform areas were repaired step by step. Additional coatings were applied by re-dipping the previously dip-coated and dried specimens at 30 °C. For each coating, a new slip was prepared every time to avoid changes in the slip particle size distribution due to the decrease in agglomeration and concentration resulting from the dip-coating procedure. The number of coatings was observed to have a strong effect on the uniformity of the overall coatings. When a substrate was coated twice with the AKP-30 slip, the coating only filled the cells of the foam, as shown in Fig. 3(a). By increasing the number of coatings to three, islands of the coating were created, covering only some areas of the substrate surface, as shown in Fig. 3(b). Upon further increasing the number of coatings to four, a uniform coating was obtained, but the coating showed cracks (Fig. 3(c)). With five coatings, the cracks were filled and a uniform coating was obtained, as shown in Fig. 3(d). Moreover, with ALM-44, a uniform coating with a smooth surface was obtained after five coatings, as shown in Fig. 3(e). It is clear that repetitious dip-coating can result in thicker films and that cracks or other defects in the initial layers can be repaired by subsequent coatings.

A cross-sectional SEM image of the fractured surface of the AKP-30 coating fabricated by the dip-coating process is shown in Fig. 4(a). A uniform coating with a thickness of 50  $\mu\text{m}$  was obtained after five dip-coatings, and no cracks were observed on the coated surface. The coating was smooth, providing a favourable surface condition. The adhesion between the coating and substrate was very strong, preventing the formation of an interlayer, and no delamination was observed, as shown in Fig. 4(b).

The AKP-30 and ALM-44 coatings with different particle sizes are compared in Fig. 5. All of the specimens were coated five times, and the coating thickness was observed to increase when the particle size of the  $\text{Al}_2\text{O}_3$  increased. The coating thickness of the specimens coated with AKP-30 was 50  $\mu\text{m}$ , whereas that of the specimens coated with ALM-44 was 140  $\mu\text{m}$ , as shown in Fig. 5(a) and (b) because a large particle size will result in a thicker coating. The fractured surface of the coatings sintered at 1600 °C shows that porous coatings were obtained, which can be used as a thermal insulation material, as

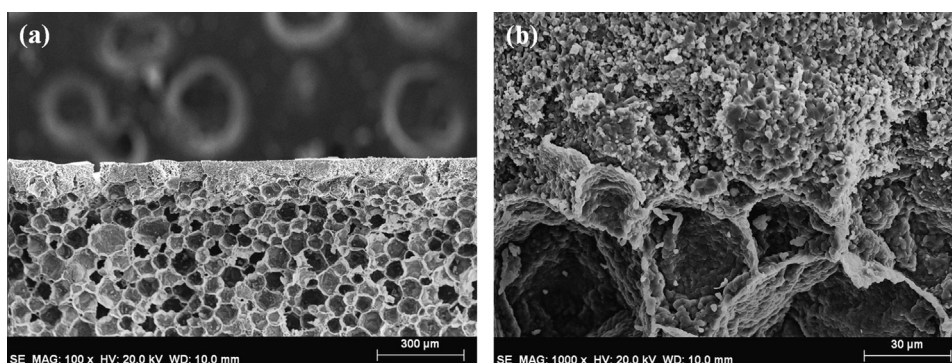


Fig. 4. SEM images of the AKP-30 coating sintered at 1600 °C for 1 h: (a) cross-section showing a uniform coating on a highly porous substrate and (b) interface between the coating layer and the substrate at a higher magnification.



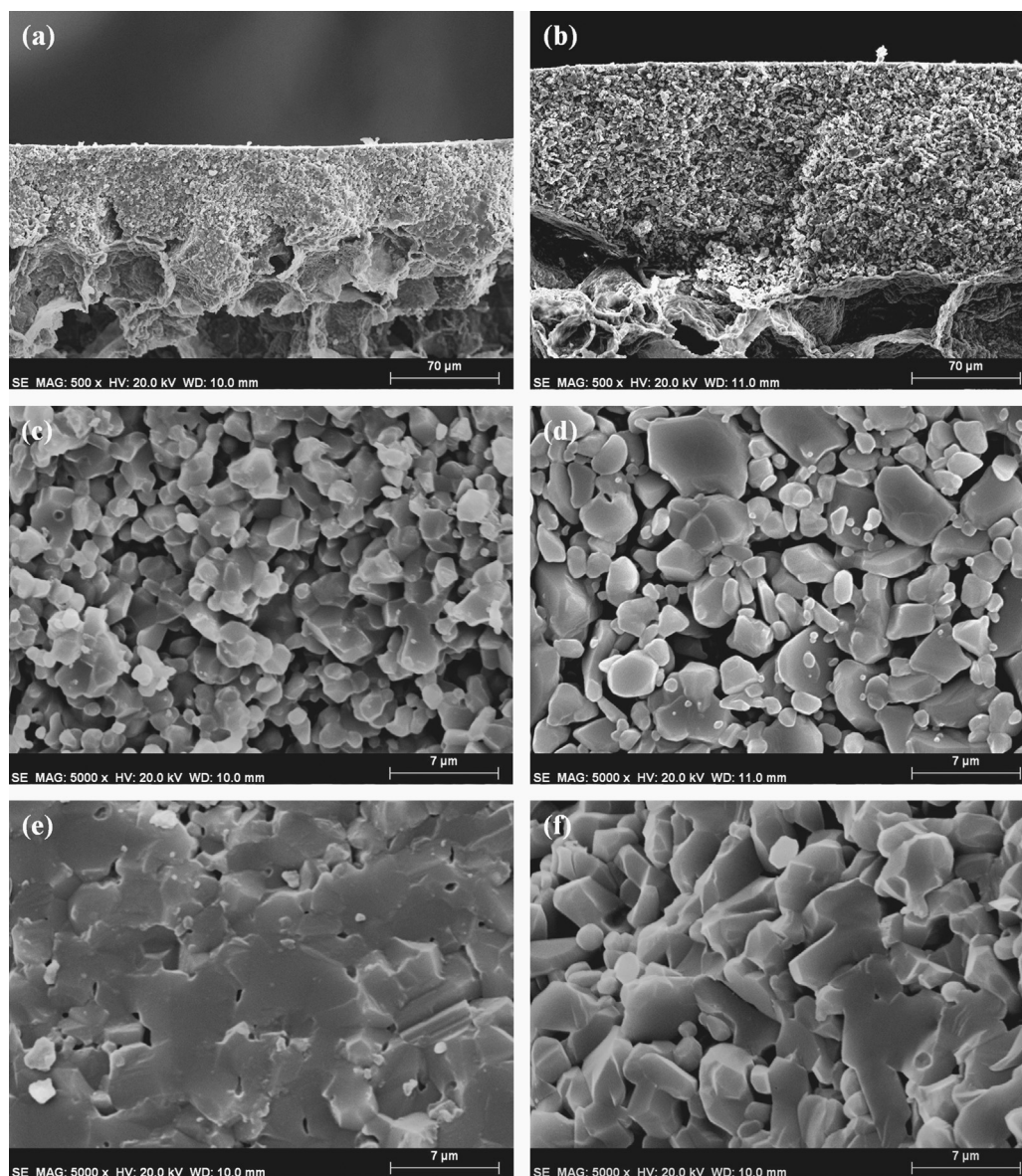


Fig. 5. SEM images of (a) the interface of the AKP-30 coating and the substrate sintered at 1600 °C for 1 h, (b) the interface of the ALM-44 coating and the substrate sintered at 1600 °C for 1 h, (c) a fractured surface of the AKP-30 coating sintered at 1600 °C for 1 h, and (d) a fractured surface of the ALM-44 coating sintered at 1600 °C for 1 h. In contrast, (e) shows a fractured surface of the AKP-30 coating sintered at 1700 °C for 1 h, and (f) shows a fractured surface of the ALM-44 coating sintered at 1700 °C for 1 h.

shown in Fig. 5(c) and (d). When the sintering temperature was increased to 1700 °C, densification along with grain growth occurred in the AKP-30 coating, as shown in Fig. 5(e), whereas densification was generally observed in the ALM-44 coating, as shown in Fig. 5(f).

The crack-healing results of the highly porous  $\text{Al}_2\text{O}_3$  foam with the ALM-44 coating sintered at 1700 °C for 1 h are shown in Fig. 6. The cracks in the highly porous  $\text{Al}_2\text{O}_3$  substrate were effectively healed with the coating, indicating that the solid loading and amount of binder added to the slip are suitable. The slip successfully penetrated into the cracks to heal them. For effective crack healing, the coating should be strongly bonded to the substrate. In our specimens, there was no delamination observed in the crack-filled area, and the coatings were strongly bonded to the substrates after sintering.

The compressive strength of  $\text{Al}_2\text{O}_3$  foam coated with AKP-30 and ALM-44 was compared with that of uncoated  $\text{Al}_2\text{O}_3$  foam sintered at 1600 °C and 1700 °C for 1 h, as shown in Fig. 7. The compressive strength of the foam coated with AKP-30 was twice that of the uncoated foam, whereas the foam coated with ALM-44 did not show a high strength despite the thicker coating relative to the thickness of the AKP-30 coating sintered at 1600 °C. AKP-30 has a small particle size  $D_{50}$  of 0.3  $\mu\text{m}$  with a narrow distribution, whereas ALM-44 has a large particle size  $D_{50}$  of 3.148 with a wide distribution. The driving force for densification is the change in the free energy caused by the decrease in the surface area and the decrease in the surface free energy caused by the replacement of solid–vapour interfaces. The sinterability of the specimens coated with AKP-30 ( $D_{50}$  0.3  $\mu\text{m}$ ) was high due to



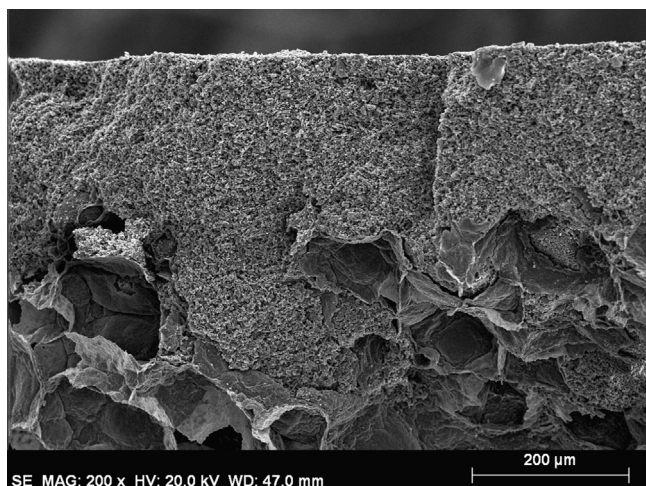


Fig. 6. SEM image of the ALM-44 coating on an  $\text{Al}_2\text{O}_3$  substrate showing crack healing after sintering at  $1700^\circ\text{C}$  for 1 h.

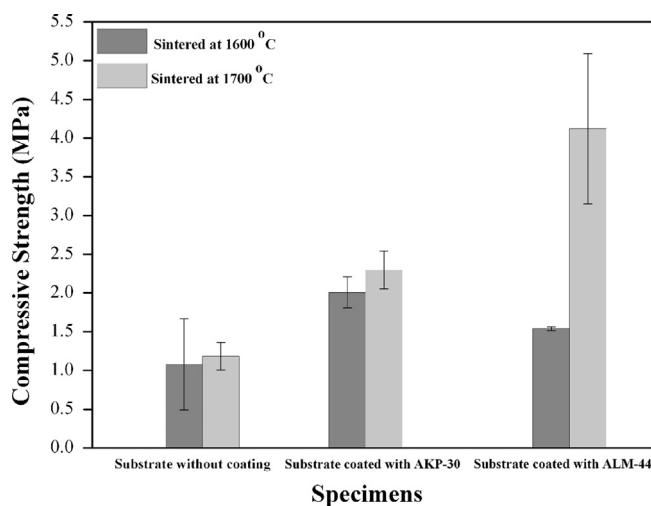


Fig. 7. Compressive strength of uncoated foam and coated foam with AKP-30 and ALM-44 sintered at  $1600^\circ\text{C}$  and  $1700^\circ\text{C}$  for 1 h.

the small initial particle size and the high surface area of the coating material, which showed a grain size of approximately  $1\ \mu\text{m}$  upon sintering at  $1600^\circ\text{C}$  (Fig. 5(c)), whereas the specimens coated with ALM-44 ( $D_{50}\ 3.148$ ) did not show good sinterability at  $1600^\circ\text{C}$  (Fig. 5(d)), resulting in a low compressive strength. When the sintering temperature was increased to  $1700^\circ\text{C}$ , there was almost no change in the compressive strength of the substrate, whereas densification in the AKP-30-coated specimens was complete and the compressive strength was slightly increased. Although densification occurred in the ALM-44 coating after the sintering temperature was increased to  $1700^\circ\text{C}$ , the effect of a thick coating is more dominant in increasing the compressive strength, as shown in Fig. 7. Thus, the optimum sintering temperature and duration for the ALM-44 coating are respectively  $1700^\circ\text{C}$  and 1 h to achieve a high compressive strength.

A schematic representation of the coating process for improving the surface condition and repairing the cracks of a highly porous substrate manufactured by the particle-stabilised direct foaming technique is shown in Fig. 8. The improvement in the substrate surface is based on the filling of inhomogeneous defects and crack healing, which thus improve the substrate's compressive strength and resistance to debris to yield an outstanding material with an ultra-high porous core and relatively less porous surface. The crack-healed  $\text{Al}_2\text{O}_3$  foam created by dip-coating shows good compressive strength and can be used as a low-weight structural, thermal, and electrically insulating material in a corrosive environment requiring good wear resistance. Furthermore, because processing cost is very important when fabricating engineering ceramics for such applications, the major advantage of this process is the ability to form complex shapes using various mould materials and low-cost processing equipment and materials.

#### 4. Conclusions

AKP-30 and ALM-44 coatings with thicknesses of  $50\ \mu\text{m}$  and  $140\ \mu\text{m}$ , respectively, were successfully fabricated on highly porous substrates with a cell size ranging from 70 to

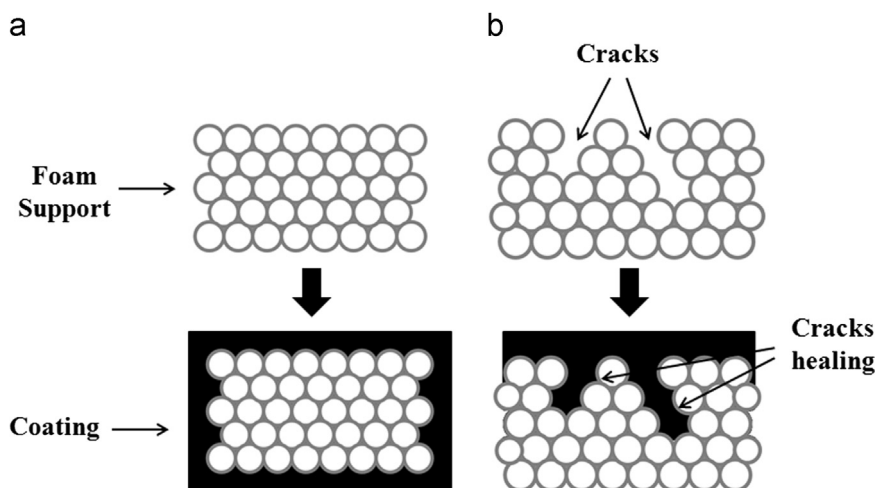


Fig. 8. Schematic of a foam coating showing (a) an improved surface condition and (b) crack healing.



200  $\mu\text{m}$  and a porosity of 90% utilising a simple dip-coating process. After sintering, the coatings exhibited good adhesion to a porous substrate without delamination. The increase in the compressive strength of porous  $\text{Al}_2\text{O}_3$  substrates afforded by the coatings was believed to be due to the healing of cracks and surface defects. The results of this study suggest that the crack healing of highly porous  $\text{Al}_2\text{O}_3$  foam by dip-coating is a potentially useful approach for enhancing the compressive strength thereof. These materials can be useful in low-weight structural applications requiring a clean environment without debris along with good compressive strength.

### Acknowledgements

This study was supported financially by the Fundamental Research Programme of the Korea Institute of Materials Science (KIMS).

### References

- [1] Y.W. Lo, W.C.J. Wei, C.H. Hsueh, Low thermal conductivity of porous alumina foams for SOFC insulation, *Materials Chemistry and Physics* 129 (2011) 326–330.
- [2] A.R. Studart, U.T. Gonzenbach, E. Tervoort, L.J. Gauckler, Processing routes to macroporous ceramics: a review, *Journal of the American Ceramic Society* 89 (2006) 1771–1789.
- [3] H.J. Son, R.H. Song, T.H. Lim, S.B. Lee, S.H. Kim, D.R. Shin, Effect of fabrication parameters on coating properties of tubular solid oxide fuel cell electrolyte prepared by vacuum slurry coating, *Journal of Power Sources* 195 (2010) 1779–1785.
- [4] W. Lan, P. Xiao, Fabrication of yttria-stabilized-zirconia thick coatings via slurry process with pressure infiltration, *Journal of the European Ceramic Society* 29 (2009) 391–401.
- [5] C. Cristiani, M. Valentini, M. Merazzi, S. Neglia, P. Forzatti, Effect of ageing time on chemical and rheological evolution in  $\gamma\text{-Al}_2\text{O}_3$  slurries for dip-coating, *Catalysis Today* 105 (2005) 492–498.
- [6] J.H. Ha, R. Ahmad, I.H. Song, A novel method of coating a particle-stabilized alumina foam on a porous alumina substrate, *Materials Letters* 88 (2012) 40–42.
- [7] C. Falamaki, M. Naimi, A. Aghaie, Dip-coating technique for the manufacture of alumina microfilters using PVA and Na-CMC as binders: a comparative study, *Journal of the European Ceramic Society* 26 (2006) 949–956.
- [8] A. Torabi, T.H. Etsell, P. Sarkar, Dip-coating fabrication process for micro-tubular SOFCs, *Solid State Ionics* 192 (2011) 372–375.
- [9] Y. Gu, G. Meng, A model for ceramic membrane formation by dip-coating, *Journal of the European Ceramic Society* 19 (1999) 1961–1966.
- [10] U.T. Gonzenbach, A.R. Studart, E. Tervoort, L.J. Gauckler, Ultrastable particle-stabilized foams, *Angewandte Chemie International Edition* 45 (2006) 3526–3530.
- [11] U.T. Gonzenbach, A.R. Studart, E. Tervoort, L.J. Gauckler, Stabilization of foams with inorganic colloidal particles, *Langmuir* 22 (2006) 10983–10988.
- [12] U.T. Gonzenbach, A.R. Studart, E. Tervoort, L.J. Gauckler, Tailoring the microstructure of particle-stabilized wet foams, *Langmuir* 23 (2007) 1025–1032.
- [13] T.N. Hunter, R.J. Pugh, G.V. Franks, G.J. Jameson, The role of particles in stabilizing foams and emulsions, *Advances in Colloid and Interface Science* 137 (2008) 57–81.
- [14] C. Chuanuwatanakul, C. Tallon, D.E. Dunstan, G.V. Franks, Controlling the microstructure of ceramic particle-stabilized foams influence of contact angle and particle aggregation, *Soft Matter* 7 (2011) 11464–11474.
- [15] G. Kaptay, Interfacial criteria for stabilization of liquid foams by solid particles, *Colloids and Surfaces A: Physicochemical and Engineering Aspects* 230 (2004) 67–80.
- [16] F.F. Lange, K.C. Radford, Healing of surface cracks in polycrystalline  $\text{Al}_2\text{O}_3$ , *Journal of the American Ceramic Society* 53 (1970) 420–421.